Heliyon 9 (2023) e18497

Contents lists available at ScienceDirect

Heliyon

journal homepage: www.cell.com/heliyon

Cuproptosis-related genes prediction feature and immune microenvironment in major depressive disorder

Daoyun Lei [a,b], Jie Sun [a,b,*], Jiangyan Xia [a,b,**]

[a] Department of Anesthesiology, Zhongda Hospital Southeast University (Jiangbei), Nanjing, 210048 Jiangsu, China
[b] Department of Anesthesiology, Zhongda Hospital Southeast University, Nanjing, 210009 Jiangsu, China

ARTICLE INFO

Keywords:
Cuproptosis
Major depressive disorder
Gene
Predictive model
RF model

ABSTRACT

Background: Major depressive disorder (MDD) is a severe, unpredictable, ill-cured, relapsing neuropsychiatric disorder. A recently identified type of death called cuproptosis has been linked to a number of illnesses. However, the influence of cuproptosis-related genes in MDD has not been comprehensively assessed in prior study.

Aim: This investigation intends to shed light on the predictive value of cuproptosis-related genes for MDD and the immunological microenvironment.

Methods: GSE38206, GSE76826, GSE9653 databases were used to analyze cuproptosis regulators and immune characteristics. To find the genes that were differently expressed, weighted gene co-expression network analysis was employed. We calculated the effectiveness of the random forest model, generalized linear model, and limit gradient lifting to arrive at the best machine prediction model. Nomogram, calibration curve, and decision curve analysis were used to show the anticipated MDD's accuracy.

Results: This study found that there were activated immune responses and cuproptosis-related genes that were dysregulated in people with MDD compared to healthy controls. Considering the test performance of the learned model and validation on subsequent datasets, the RF model (including OSBPL8, VBP1, MTM1, ELK3, and SLC39A6) was considered to have the best discriminative performance. (AUC = 0.875).

Conclusion: Our study constructed a prediction model to predict MDD risk and clarified the potential connection between cuproptosis and MDD.

1. Introduction

A recurrent depressive condition with severe physical and psychological symptoms is known as major depressive disorder (MDD) [1]. Major depressive disorder was identified using the Diagnostic and Statistical Manual of Mental Disorders (DSM-5) as follows: 5 or more near-daily bouts of any symptom for two weeks on the premise of at least one underlying condition [2]. The World Health Organization surveyed 14 countries or regions and found that while methodological differences can lead to significant differences in

* Corresponding author. Zhongda Hospital Southeast University, No.211, Jianmin Road, Nanjing, China.
** Corresponding author. Zhongda Hospital Southeast University, No.211, Jianmin Road, Nanjing, China.
E-mail addresses: dgsunjie@hotmail.com (J. Sun), jiangyanxia731026@aliyun.com (J. Xia).

https://doi.org/10.1016/j.heliyon.2023.e18497
Received 2 February 2023; Received in revised form 17 July 2023; Accepted 19 July 2023
Available online 26 July 2023

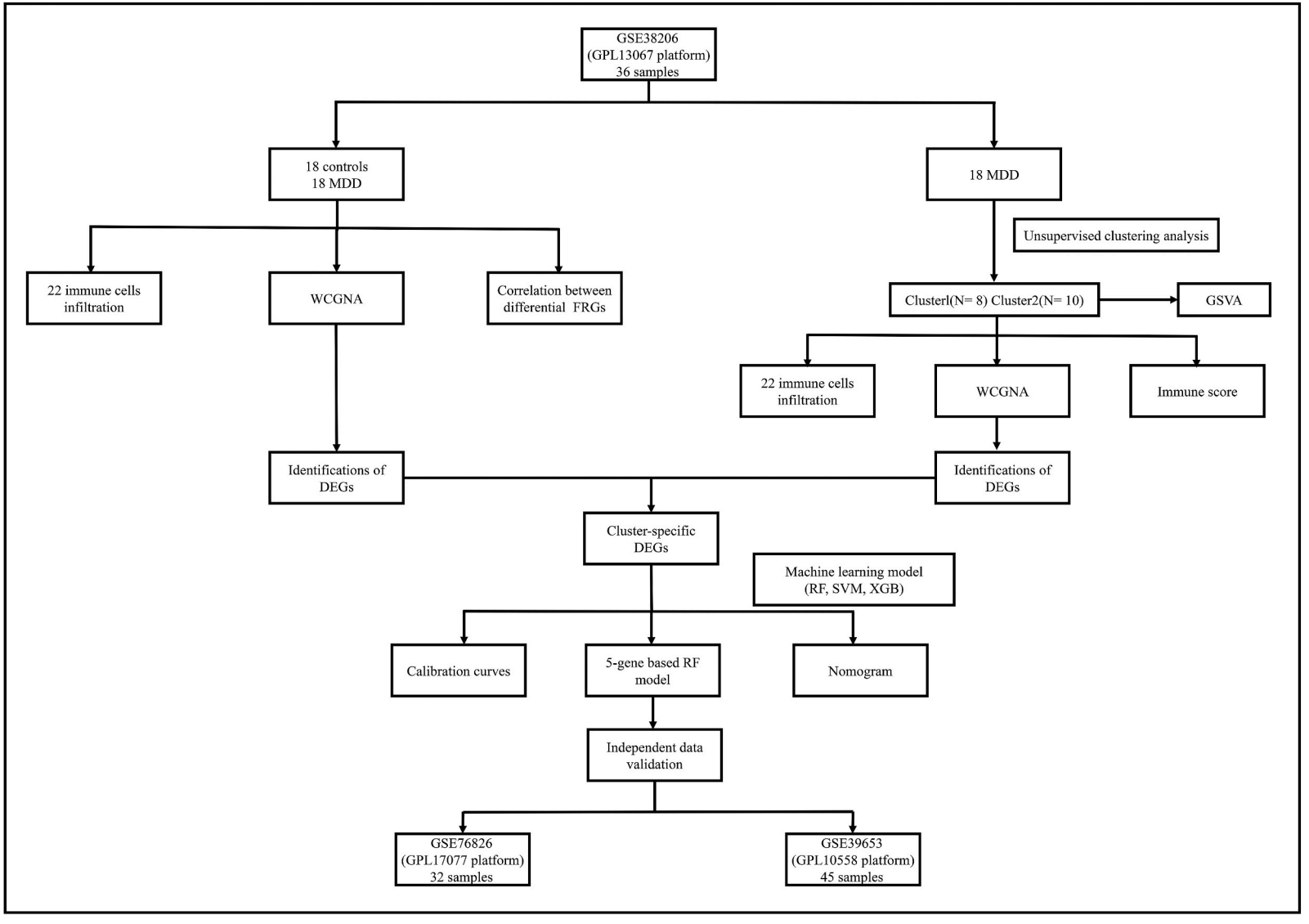

Fig. 1. The flow chart of this study.

national estimates of lifetime prevalence and disease duration, the high risk of chronic relapses from MDD is clear [3]. An epidemiological study on the prevalence of major depressive illness among people in the United States was carried out by Deborah S. Hasin et al. They discovered that the lifetime prevalence of MDD was 20.6% and the 12-month prevalence was 10.4%, elucidating the true incidence of MDD and addressing the gap in the MDD literature caused by the lack of US national databases [4]. Highly heterogeneous, multifactorial, and high incidence characteristics make diagnosing or treating major depressive disorder challenging. The underlying mechanisms of major depression have been advanced, but no perfect mechanism can satisfactorily explain all aspects of the disease due to the variable duration, frequency, and pattern of episodes. Therefore, discovering mechanisms derived from the biological underpinnings provided directly by clinical studies is crucial to identifying new diagnostic indicators and therapeutic targets for patients.

Copper, an essential element in the human body, is critical for maintaining the stability of the physical microenvironment. As an essential micronutrient, copper is required for various physiological processes in almost all cell types. Although copper is an important enzyme cofactor, slightly abnormal intracellular concentrations can be toxic and lead to cell death. Therefore, the body strictly regulates the uptake, distribution, and elimination of copper and maintains a dynamic balance. Any factor leading to copper accumulation in the human body can cause serious and potentially life-threatening pathological conditions. Since intracellular copper accumulation causes oxidative stress and disrupts cellular functions, leading to non-apoptotic programmed cell death by binding to small molecule chaperones, this copper ion-induced cell death group is non-apoptotic, non-ferrous, and non-necrotic [5,6]. This new form of copper-dependent cell death is called cuproptosis. The onset of copper toxicity depends on TCA's fatty acid polymerization protein circulating in active cells and the subsequent acute proteotoxic stress that disrupts mitochondrial metabolism. Excessive copper concentrations are associated with the development of MDD. Recent studies have also found that abnormal concentrations of copper induce cell death and disrupt synaptic function or neural metabolism, leading to memory impairment in depressed patients [7,8]. These studies imply a role in cuproptosis in MDD, yet direct evidence is still lacking. We used bioinformatics techniques to elucidate the potential association of cuproptosis with MDD through existing datasets. In addition, MDD still lacks a valid predictive model, and we also attempted to build reliable predictive models. Thus, elucidating the underlying mechanisms of major depressive disorder by exploring physiological and pathological activities is crucial for early diagnosis and effective therapeutic targets.

This study explored immune signatures and CRGs (cuproptosis-related genes) between normal and MDD individuals according to three GEO datasets. The expression patterns of 19 CRGs were used to assess the differences in immune cell penetration between the two cuproptosis-related clusters after the construction of two of them. The WGCNA-identified cluster-specific DEGs were then used in a matching functional analysis. While this is happening, a patient prediction model is created by contrasting several machine learning techniques. The flowchart of this study is shown in Fig. 1.

2. Methods

2.1. Data processing and download of the MDD dataset

Datasets GSE38206, GSE76826, and GSE39653's gene expression profiles were retrieved from the GEO database at https://www.ncbi.nlm.nih.gov/geo/query/acc.cgi?acc=GSE38206, GSE76826, and GSE39653, respectively. These data were detected by the platforms Agilent-028004 SurePrint G3 Human GE 8 × 60K Microarray (Feature Number version), Agilent-039494 SurePrint G3 Human GE v2 8 × 60K Microarray 039381 (Probe Name version), and Illumina HumanHT-12 V4.0 expression beadchip, respectively. The GSE38206 dataset was selected for further analysis, containing the mRNA expression data of PBMCs from 18 normal individual samples and 18 MDD samples. The GSE76826 dataset comprises the PBMCs mRNA expression data of 12 normal individual samples and 20 MDD samples. The GSE39653 dataset comprises the whole blood mRNA expression data of 24 normal individual samples and 21 MDD samples, both of which were selected for validation analysis. Specific information is shown in Table 1. Data mining and statistical analysis depend on R software (version 3.6.1) and Bioconductor Packages (version 3.10) [9]. These differential expression genes (DEGs) were recognized with the limma package in R [10]. We used the R programs "ggplot2″ and "pheatmap" to create heatmaps and volcano plots from the data, respectively. Because only published data was used in this study, no ethical approval was required.

Table 1
The summary of GEO datasets used in the present study.

GEO accession	Platform	Samples	Patients subgroup	Sample source
GSE38206	GPL13607	36	18 control samples and 18 MDD samples	PBMC
GSE76826	GPL17077	32	12 control samples and 20 MDD samples	blood
GSE39653	GPL10558	53	24 control samples, 21 MDD samples and 8 BD samples	PBMC

GEO: Gene Expression Omnibus data base, MDD: major depressive disorder, PBMC: Peripheral blood mononuclear cell, BD: bipolar disorder.

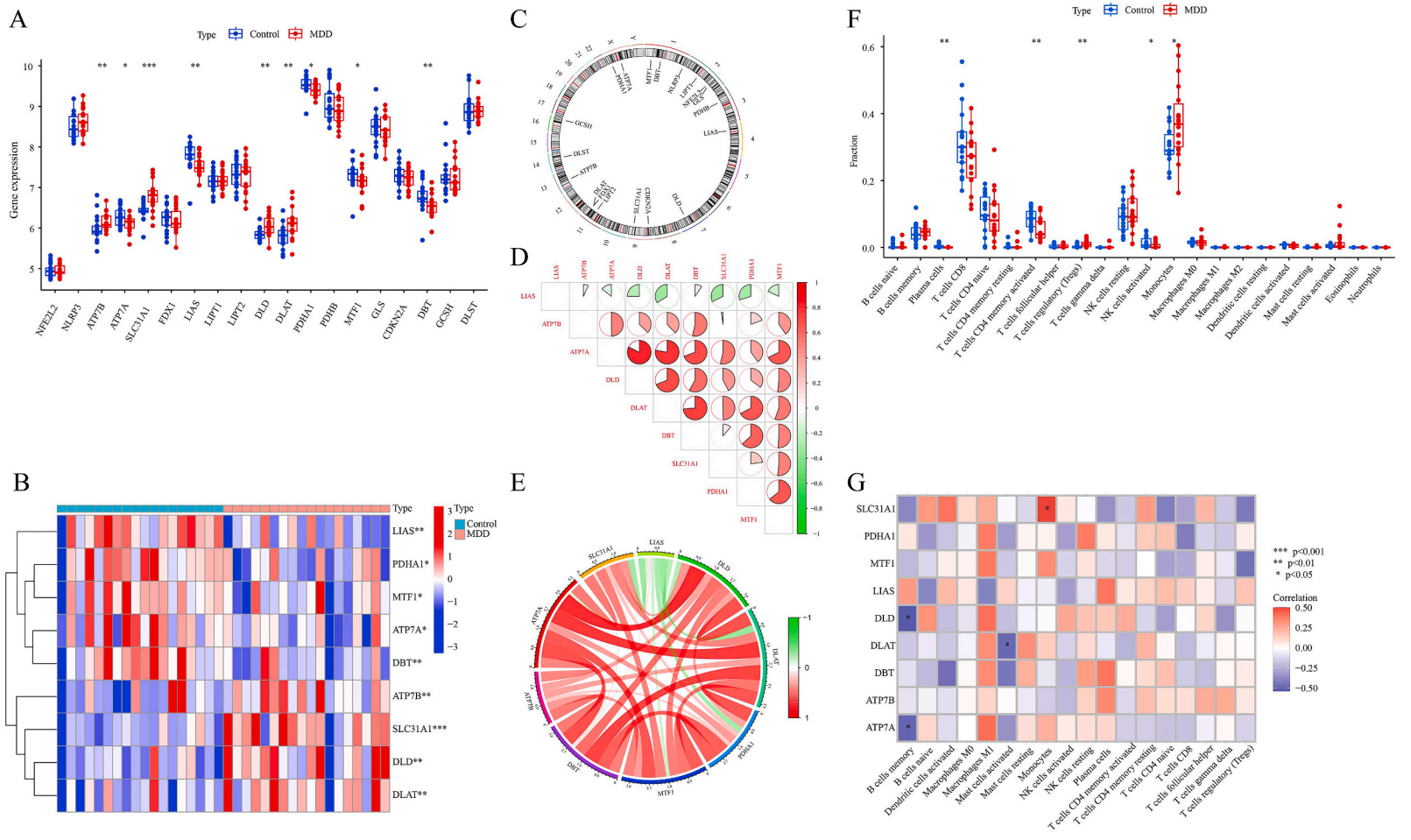

Fig. 2. 19 CRGs (cuproptosis-related genes) express themselves differently in people with MDD and healthy people. (A)The boxplots showed the expression of 19 CRGs. (B)Heatmap differential level is reflected by CRGs with differential expressions.(C)The locations of each chromosome's 19 associated CRGs. (D,E)Diagram of the gene connection network and correlation study of nine CRGs with varied levels of expression. Positive and negative correlations are represented by the colors red and green, respectively. (F)The differences in immunological infiltration between MDD and healthy individual controls were displayed in boxplots. (G) Investigation of the relationships between infiltrating immune cells and 12 differentially expressed CRGs. *p < 0.05, ***p < 0.001, ****p < 0.0001. (For interpretation of the references to color in this figure legend, the reader is referred to the Web version of this article.)

2.2. Analysis of correlation and evaluation of immune cell infiltration

Using the CIBERSORT algorithm and the LM22 feature matrix based on gene expression data, the relative abundances of the 22 immune cell types in the sample were calculated. *P*-value <0.05 is the criterion for an accurate immune cell composition. By adding the fraction of 22 immune cells in each sample to one, accuracy validation was assessed. The "corrplot" R software and the Spearman correlation coefficient (p-value$<$ 0.05 indicated a significant link) showed an association between CRG and immune cell features related to MDD [11].

2.3. Unsupervised clustering of MDD patients

Conveniently, nineteen genes related to cuproptosis were obtained from the published literature [5,12]. MDD samples were classified into different clusters by applying unsupervised cluster analysis and k-means algorithm. First, we followed Yongxing Lai et al. [13] and picked the highest amount of subtypes possible, k (k = 9) [13]. The optimum amount of clusters (>0.9) was determined by combining consensus cluster scores, consensus matrices, and composite cumulative distribution function curves.

2.4. Gene set variation analysis (GSVA) analysis

The R package "GSVA" was used to perform GSVA analysis on the route differences of CRGs clusters. The biological functions and pathways with differential expression were found using the "limma" R tool. A statistically significant change has a t-value greater than 2.

2.5. Analysis of the weighted gene co-expression network (WGCNA)

WGCNA algorithm was performed to analyze the co-expression networks in DEGs between MDD and controls [14]. A weighted adjacency matrix was then created after calculating a sufficient soft threshold β using a weighted correlation adjacency matrix and cluster analysis. The topological overlap matrix (TOM) of the resulting matrix was transformed to provide the equivalent dissimilarity (1-TOM). Hierarchical clustering of genes and subsequent dendrogram visualization derived from dissimilarity TOM. Relationships between clinical traits and module eigengenes were assessed with Pearson's r correlation.

2.6. Construction of suitable predictive models

Three machine learning models dubbed Random Forest (RF), Extreme Gradient Boosting (XGB), and Generalized Linear Model (GLM) were developed by "caret" R packages to further evaluate the two distinct CRG clusters. These models' parameters are automatically adjusted for grid search during training using the caret package. With default settings, these models were run and cross-validated for evaluation. The models were thoroughly evaluated using the "DALEX" package, which also served to display the performance variations, residual distributions, and feature weights of several prediction models. In the end, the most effective machine learning model and significant predictor genes were discovered.

2.7. Construction and verification of nomogram

The "rms" R package was utilized to create a nomogram model to evaluate the occurrence of MDD clusters. Each predicted gene has a visualized score and calculates the total score. Calibration curves and DCA were used to the GSE76826 and GSE39653 datasets in order to better demonstrate the nomogram model's predictive ability.

3. Results

3.1. Cuproptosis gene expression and immune cell infiltration in MDD patients

We compared the expression of 19 CRGs between healthy individual controls and MDD using the GSE38206 dataset, illuminating the biological role of the cuproptosis-related genes in the onset and progression of MDD. We discovered nine cuproptosis genes that were differently expressed in accordance with the flowchart in Fig. 1. As shown in Fig. 2A–C, the expression levels of the genes ATP7B, SLC31A1, DLD, and DLAT were higher in the MDD group, whereas those of ATP7A, LIAS, PDHA1, MTF1, and DBT were lower. We conducted a correlation analysis on these differentially expressed CRGs to examine the critical role of the cuproptosis regulators in MDD. These findings revealed that various cuproptosis modulators, including ATP7A and DLAT (coefficient = 0.86), LIAS and DLAT (coefficient = 0.38), had synergistic or antagonistic effects. DLAT and ATP7A were found to be significantly related with other regulators after analysis of these CRG association patterns, and gene-relation network plots (Fig. 2D and E) were used to demonstrate the degree of association.

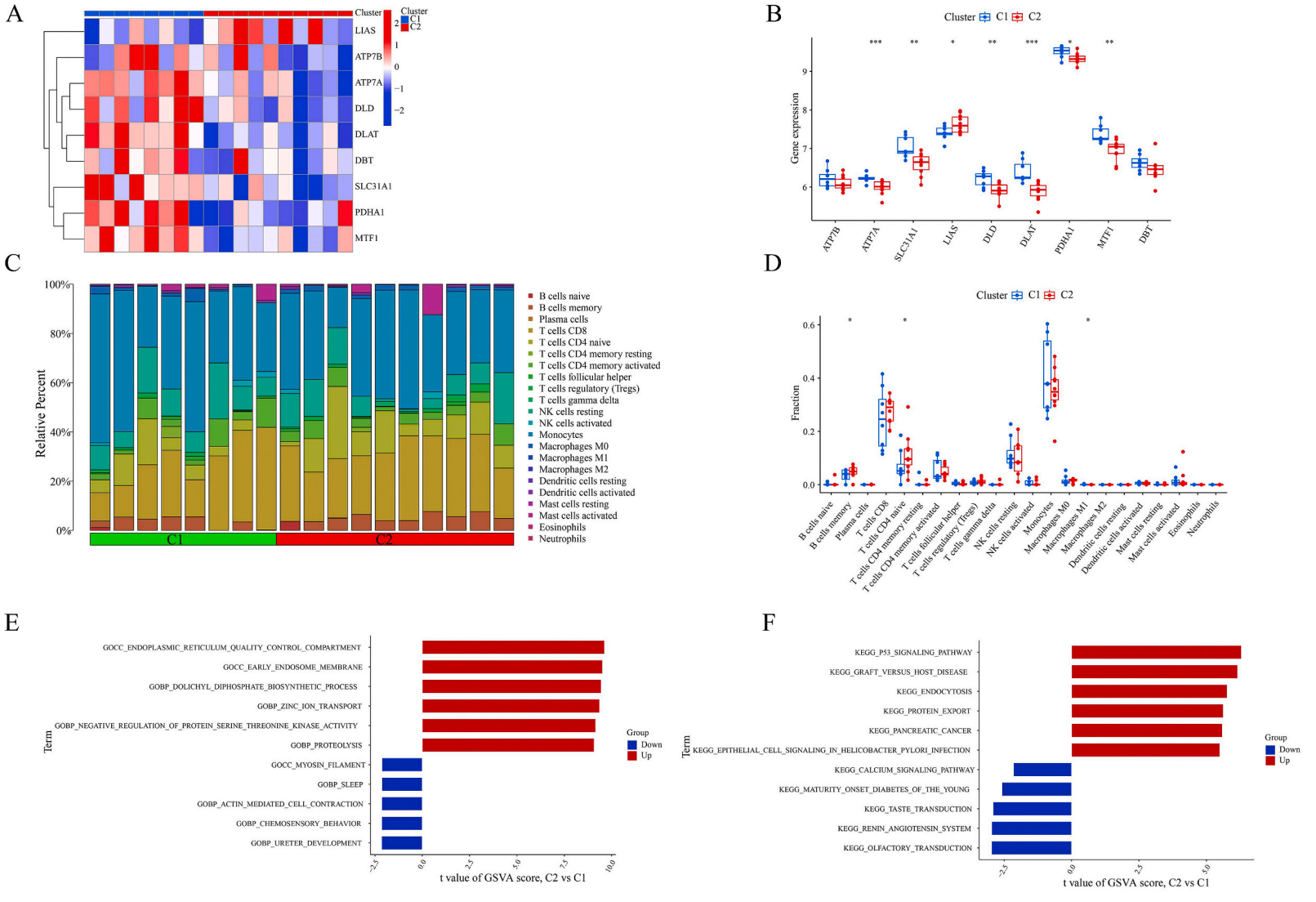

Fig. 3. Molecular and immunological traits that distinguish the two cuproptosis clusters. (A)The heatmap displayed the expression of the two cuproptosis clusters. (B)The differential level in the boxplots is reflected in CRGs with differential expressions. (C)22 immune cells that infiltrate between the two cuproptosis clusters in according to their abundance. (D)The variations in immune infiltration between the two cuproptosis clusters were displayed using boxplots. (E,F)Pathway variations across several CRGs clusters were analyzed using Gene Set Variation Analysis (GSVA). *$p < 0.05$, ***$p < 0.001$, ****$p < 0.0001$.

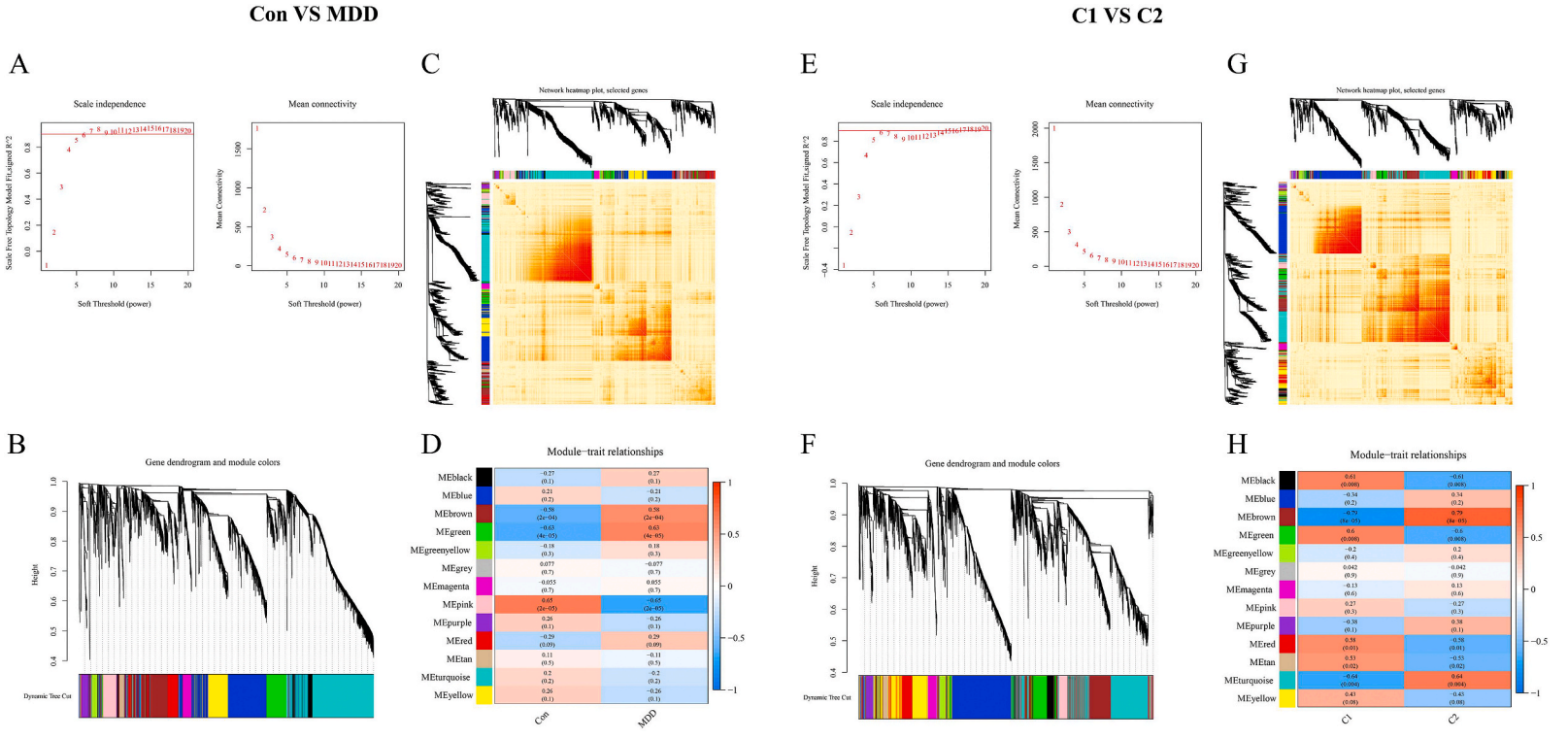

Fig. 4. Using WCGNA (weighted gene co-expression network analysis), gene modules were screened and co-expression networks were built in two clusters associated with cuproptosis and MDD. The choice of soft threshold power is in (A,E). (B,F) Co-expression module cluster tree dendrogram. Different hues stand for various co-expression modules. (C,G) A heatmap showing the correlations between the 10 modules. (D,H) Analysis of the correlation between the clinical status and the module eigengenes. Each column denotes a clinical status, whereas each row denotes a module.

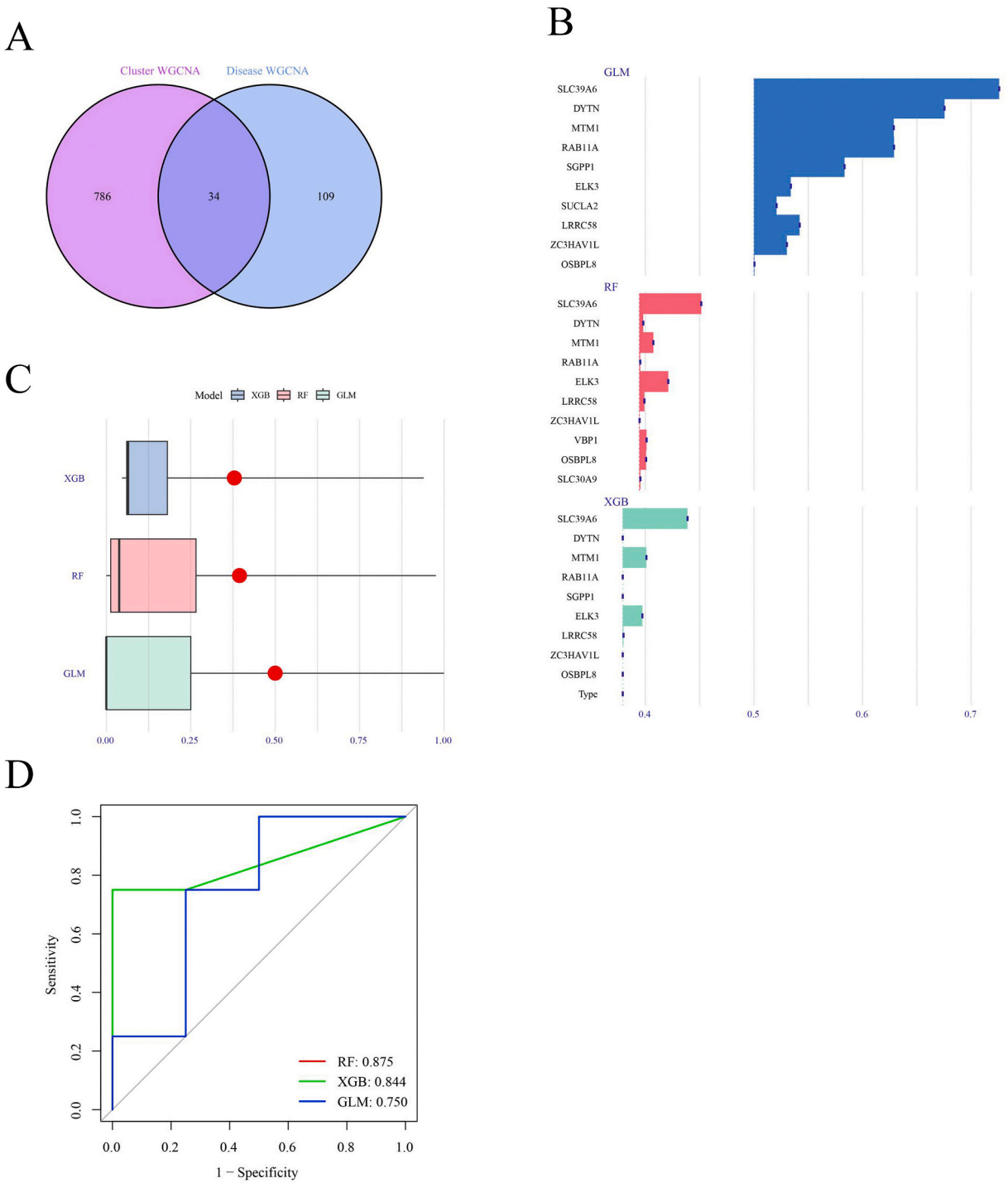

Fig. 5. Building and assessing RF, GLM, and XGB machine models. (A) The intersection of the MDD module-related genes and the cuproptosis cluster is depicted in a Venn diagram using data from the GSE38206 dataset. (B)A list of significant eigengenes for the RF, GLM, and XGB machine models. (C) Boxplots are used to display residuals for each machine learning model. The root mean square error (RMSE) of the residuals is represented by the red dots. (D) Three machine learning models' ROC analyses. (For interpretation of the references to color in this figure legend, the reader is referred to the Web version of this article.)

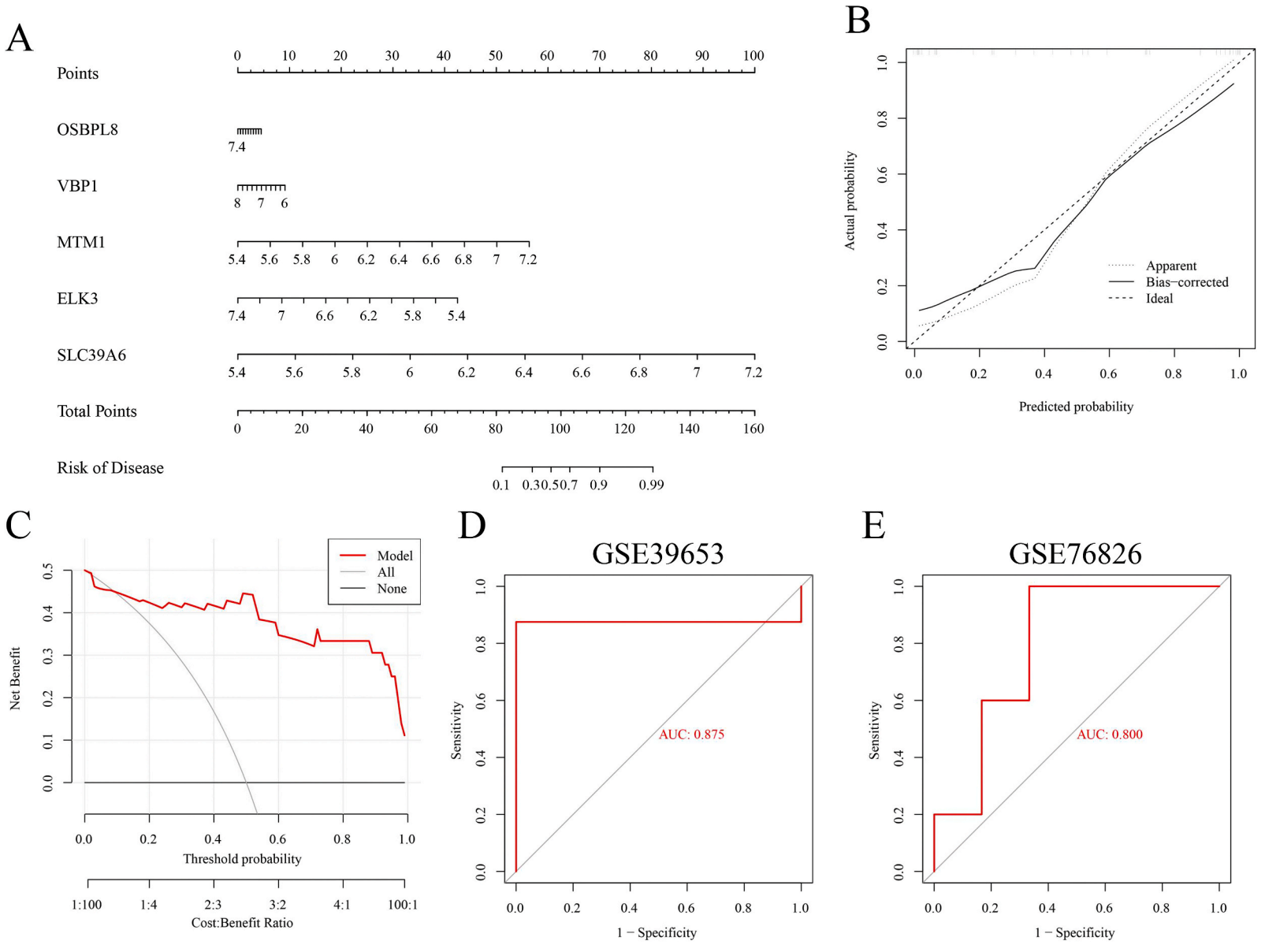

Fig. 6. Validation of the RF model based on five genes. (A) Building a nomogram based on the 5-gene RF model to estimate the risk of MDD clusters. (B,C) Building a calibration curve (B) and performing a decision curve analysis (DCA) (C) to determine how well the nomogram model predicts the future. 5-fold cross-validation was used to analyze the receiver operating characteristic curve (ROC) of the 5-gene-based RF model in the datasets GSE39653 (D) and GSE76826 (E).

The CIBERSORT algorithm was used to conduct the immune infiltration analysis in order to clarify the immune system variations between MDD and healthy controls. According to the findings, patients with MDD had higher levels of Treg infiltration and monocytes and lower levels of plasma cell infiltration, T cell CD4 memory activation, NK cell activation, and NK cell activation (Fig. 2F). According to correlation analysis, cuproptosis regulators were linked to B cell memory, activated master cells, and monocytes (Fig. 2G). The molecular and immune infiltration status in MDD patients may be significantly influenced by CRGs.

3.2. Identification of cuproptosis clusters in MDD

In order to clarify the expression patterns connected to cuproptosis in MDD, we used a consensus clustering algorithm. We discovered that for k = 2, the number of clusters was the most stable, and the fluctuations in the CDF curves were the least (Figure S1A–C). Additionally, when k = 2 (Figure S1D), the concordance for each subtype was highest. Finally, it is separated into clusters 1 (n = 8) and 2 (n = 10) using the consensus matrix's heatmap. PCA was also used to determine the significant difference between the two clusters (Figure S1E).

3.3. Differences in cuproptosis regulators and immune infiltration signatures in cuproptosis clusters

By evaluating the expression differences of nine CRGs between Cluster1 and Cluster2, molecular signatures were observed in the two cuproptosis patterns (Fig. 3A). These results showed that ATP7A, SLC31A1, DLD, DLAT, PDHA1, and MTF1 were highly expressed in cuproptosis Cluster1, while LIAS was highly expressed in cuproptosis cluster2 (Fig. 3B). As shown in Fig. 3C and D, Cluster1 presented lower levels of B cell memory, T cell naive, and higher levels of macrophages. After 19 CRGs between Cluster1 and Cluster2 were used to gene set enrichment analysis, we found that Cluster1 was prominently associated with immune -related stress response, such as P53 signal pathway, renin-angiotensin system, calcium signal pathway, graft versus host diseases and endocytosis while Cluster2 was strengthened by the import of RNA into mitochondria, localization of proteins to the Golgi apparatus, lateral part of the cell, protein localization, and protein localization. (Fig. 3E).

3.4. Gene modules screening and co-expression network construction

To find important gene modules linked to MDD, the WGCNA algorithm constructs co-expression networks and modules. We discovered that co-expressed gene modules could be identified when the soft power value was 6 and the scale-free R2 was equal to 0.9 after selecting the top 25% of the genes in GSE38206 with the highest variance for further analysis (Fig. 4A). The topological overlap matrix (TOM) heatmap, which was produced by the dynamic cutting technique, displays 13 different co-expression modules in various hues (Fig. 4B and C). Based on the similarity and adjacency of co-expression of clinical features within the gene analysis module, the pink module with 323 genes revealed the most significant relationship to MDD (Fig. 4D). The cuproptosis cluster's important gene modules were also subjected to the same approach. With = 6 and R2 = 0.9, the scale-free network was built (Fig. 4E). Fig. 4F and G shows a heatmap of the TOM of 13 modules encompassing 6861 genes. The turquoise module (1457 genes) and the MDD cluster had the strongest connection (Fig. 4H).

3.5. Construction and assessment of machine learning models

Three validated machine learning models (RF, GLM, XGB) were developed based on the expression profiles of 34 in the cuproptosis cluster and the MDD cluster to find subtype-specific genes with high diagnostic values (Fig. 5A). The top 10 significant feature variables were determined using the root means square error (RMSE) (Fig. 5B). According to the residuals distribution derived from the "DALEX" software, the RF and GLM machine learning models have comparatively low residuals (Fig. 5C). Furthermore, receiver operating characteristic (ROC) curve calculations were used to assess the discriminative effectiveness of the four machine learning algorithms. The highest area under the ROC curve (AUC) was shown by the machine learning models RF, GLM, and SVM (RF, AUC = 0.875; GLM, AUC = 0.750; XGB, AUC = 0.844, Fig. 5D). The final findings demonstrated that the RF model was the most effective and chose the top five significant variables (OSBPL8, VBP1, MTM1, ELK3, and SLC39A6) as predictor genes.

To calculate the likelihood of cuproptosis clusters in MDD patients, we created a nomogram (Fig. 6A). The prediction effectiveness of the nomogram model was evaluated using calibration curves and decision curve analysis (DCA). A nomogram with high accuracy can serve as a foundation for clinical decisions because it was discovered that the difference between the actual MDD cluster risk and the anticipated risk was minuscule (Fig. 6B and C). We then verified two outside datasets. The results indicated that our diagnostic model successfully separates people with MDD from healthy individuals, with an AUC value of 0.875 in the GSE39653 dataset and 0.800 in the GSE76826 dataset (Fig. 6D and E).

4. Discussion

Major depressive disorder, a common mental illness, has become a global health challenge. It affects 350 million people worldwide and exposes them to the risk of disability. Although doctors provide a variety of psychological and medication treatments, the identification and cure rates for major depressive disorder remain unsatisfactory [15,16]. The high degree of heterogeneity and multifactorial nature makes the existing pathological mechanisms inadequate to fully explain MDD, which also increases the difficulty in finding good drug targets. Recent studies have shown that copper ions may be one of the key trace elements in the neurobiological mechanisms of depression, as it is involved in many aspects of neurobiology and the biochemical mechanisms of antidepressants [7,17]. The major depressive disorder has been linked to high levels of copper, particularly cognitive decline and anhedonia in patients with the major depressive disorder [7]. Although copper is the essential element that sustains the body's vital activities, excessive accumulation of copper in cells can still lead to cell death, which may also be one of the triggers for depression [5,18]. Tsvetkov et al. have named a copper-dependent form of cell death "copper proptosis" that disrupts mitochondrial respiration through the accumulation of lipid mitochondrial enzymes [5]. However, the specific mechanisms of cuproptosis and its regulatory role in MDD have not been well studied, so we sought to elucidate the particular role of cuproptosis-related genes in MDD phenotype and immune microenvironment. Additionally, we attempted to find gene signatures associated with cuproptosis that could be used to predict MDD subtypes.

We speculated that MDD was related to copper poisoning and that genes associated with cuproptosis may benefit clinicians in the early diagnosis and prediction of MDD. To test this conjecture, we initially comprehensively examined the expression profiles of cuproptosis regulators in the brain tissue of normal individuals and MDD patients. The analysis showed that significantly more dysregulated CRGs were found in MDD patients than in normal individuals, suggesting that CRGs may be involved in the occurrence of MDD and play an unknown role. To reveal the underlying correlations, we found significant synergistic or antagonistic effects among cuproptosis regulators such as ATP7A, SLC31A1, DLD, DLAT, PDHA1, MTF1, and LIAS by calculating the correlation between CRG based on data from normal individuals and MDD patients. Additional calculations also found that patients with MDD exhibited lower plasma cell infiltration, T cell CD4 memory activation, NK cell activation, and higher levels of Tregs infiltration, monocytes, as confirmed by previous studies validated in blood or brain tissue [19–22]. In addition, we classified two cuproptosis -related clusters based on different cuproptosis-dependent regulatory patterns in the CRG expression profiles of MDD patients for further analysis of the effects on immune cell infiltration and related pathways. The two groups of cuproptosis-related clusters showed differences in B-cell memory, master cell activation, and monocytes, suggesting that changes in the immune environment were involved. We chose to discard the GSE76826 and GSE39653 data set as the training set because the careful consideration of subsequent model predictions is to obtain more accurate prediction results rather than these data set is not important.

Although the high incidence and heterogeneity of MDD are responsible for the difficulty in predicting prevalence, previous studies have still attempted to build practical and rigorous predictive models for accurate prediction [23–26]. As described in the review by Jie Tan et al. this results in lower model error rates and more reliable results, even though the relationships between variables are considered when building multivariate analysis models. Unfortunately, only one study has been externally validated [23]. To establish an accurate prediction model, we compared the prediction performance of machine learning methods (RF, GLM, and XGB). We combined multiple external validation datasets to define the RF machine prediction model (AUC = 0.875), which shows that RF based machine learning performs satisfactorily in predicting MDD. Of course, the effectiveness of the SVM and GLM prediction models in the test cohort is similar to the results of the RF prediction model, but for the prediction effect of the validation set predictions, the RF prediction model performs better. The RF model consists mainly of five essential variables, including OSBPL8, VBP1, MTM1, ELK3, and SLC39A6. Von Hippel-Lindau binding protein 1 (VBP1), a subunit of the folded protein complex, participates in the protein degradation pathway by targeting the α subunit of the hypoxia-inducible factor with VHL for proteasome-mediated degradation [27]. In addition, it activates NF-KB signaling, which may also be a potential mechanism for MDD exacerbation through monocyte-induced inflammatory signaling [28]. As an endocytic GAG receptor associated with nervous system development, FIBCD1 may be a potential target for the treatment of MDD [29]. Myotubulin (MTM1) 1 plays an important role in intracellular membrane trafficking and regulates autophagy by regulating PtdIns3P levels, an important substrate in the initiation phase of phagocytes [30]. Alleviating MDD by alleviating the autophagy pathway is a viable potential therapeutic approach [31]. ELK3 is a transcription factor containing an ETS domain, which regulates the expression of various genes by forming a ternary complex transcription factor (TCF) and binding to a specific DNA sequence. ELK3 is a transcription factor containing an ETS domain, which regulates the expression of various genes by forming a ternary complex transcription factor (TCF) and binding to a specific DNA sequence, and participates in depression by regulating the Wnt/β-Catenin signaling pathway [32]. Validation of the 5-gene-based RF model on two external validation datasets showed that the model is able to predict MDD accurately and successfully constructed a nomogram model for MDD diagnosis.

Some limitations of the study should not be overlooked. Our current study used bioinformatics analyses such as DEGs, WGCNA, and machine learning methods. Although different datasets were used for the validation analysis, on the one hand, we used small sample sizes, which may be somewhat biased, and on the other hand, additional clinical or experimental evaluations for validation are also indispensable. Furthermore, our results are only based on published data, and more detailed clinical characteristics are needed to confirm the predictive model's performance.

5. Conclusion

Overall, we have explored the association of CRGs with MDD patients and immune percolation in a multifaceted manner through various bioinformatics approaches. Based on the above results, we find that the RF model can more accurately predict the occurrence of MDD and explain the possible underlying mechanisms of MDD. Therefore, an appropriate cuproptosis score may have clinical benefits for the early identification of MDD, but more clinical studies are needed to verify this.

Declarations

Author contribution statement

Jie Sun: Conceived and designed the experiments; Performed the experiments; Analyzed and interpreted the data; Contributed reagents, materials, analysis tools or data; Wrote the paper.

Daoyun Lei: Analyzed and interpreted the data; Wrote the paper.

Jiangyan Xia: Analyzed and interpreted the data; Contributed reagents, materials, analysis tools or data.

Funding statement

National Natural Science Foundation of China, Grant/Award Numbers: No.82201346.

National Natural Science Foundation of China, Grant/Award Numbers: No.82071196.

Data availability statement

The datasets generated and analyzed during the current study are available from https://www.ncbi.nlm.nih.gov/geo/.

Additional information

No additional information is available for this paper.

Declaration of competing interest

The authors declare that they have no known competing financial interests or personal relationships that could have appeared to influence the work reported in this paper.

Appendix

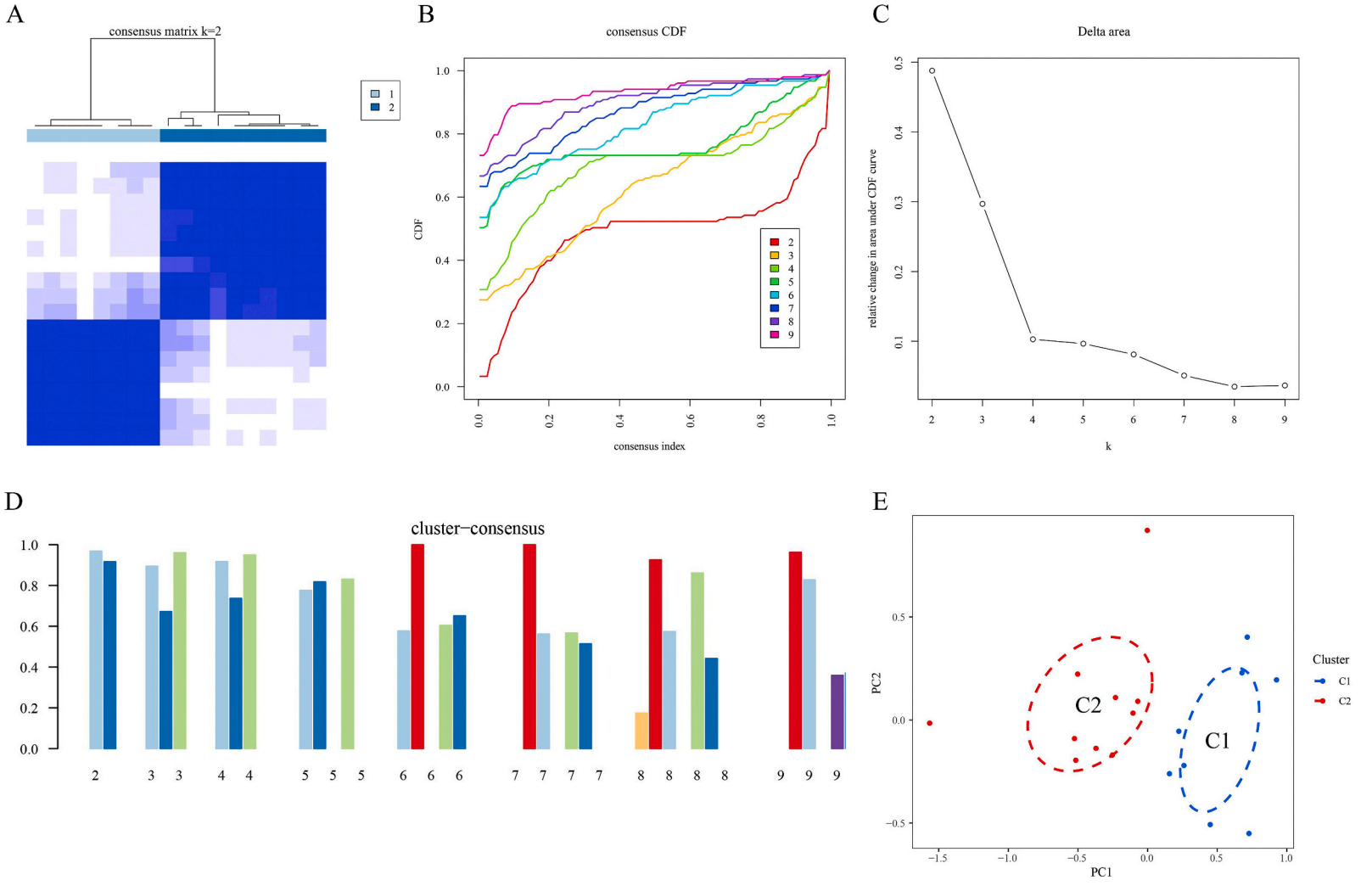

Figure S1. Identification of cuproptosis-related molecular clusters in CRDs. (A) Consensus clustering matrix when k = 2.(B)Representative cumulative distribution function (CDF) curves ,(C) CDF delta area curves , (D)the score of consensus clustering,(E) difference between the two clusters was determined by PCA(Principal Component Analysis).

References

[1] G.S. Malhi, J.J. Mann, Depression, Lancet 392 (10161) (2018) 2299–2312.
[2] T.A. Widiger, A. Hines, The diagnostic and statistical manual of mental disorders, fifth edition alternative model of personality disorder, Per. Disord. 13 (4) (2022) 347–355.
[3] R.C. Kessler, E.J. Bromet, The epidemiology of depression across cultures, Annu. Rev. Publ. Health 34 (2013) 119–138.
[4] D.S. Hasin, A.L. Sarvet, J.L. Meyers, T.D. Saha, W.J. Ruan, M. Stohl, B.F. Grant, Epidemiology of adult DSM-5 major depressive disorder and its specifiers in the United States, JAMA Psychiatr. 75 (4) (2018) 336–346.
[5] P. Tsvetkov, S. Coy, B. Petrova, M. Dreishpoon, A. Verma, M. Abdusamad, J. Rossen, L. Joesch-Cohen, R. Humeidi, R.D. Spangler, et al., Copper induces cell death by targeting lipoylated TCA cycle proteins, Science 375 (6586) (2022) 1254–1261.
[6] E.J. Ge, A.I. Bush, A. Casini, P.A. Cobine, J.R. Cross, G.M. DeNicola, Q.P. Dou, K.J. Franz, V.M. Gohil, S. Gupta, et al., Connecting copper and cancer: from transition metal signalling to metalloplasia, Nat. Rev. Cancer 22 (2) (2022) 102–113.
[7] Z. Li, G. Wang, S. Zhong, X. Liao, S. Lai, Y. Shan, J. Chen, L. Zhang, Q. Lu, S. Shen, et al., Alleviation of cognitive deficits and high copper levels by an NMDA receptor antagonist in a rat depression model, Compr. Psychiatr. 102 (2020), 152200.
[8] J. Slupski, W.J. Cubala, N. Gorska, M. Galuszko-Wegielnik, M.S. Wiglusz, Role of copper in depression. Relationship with ketamine treatment, Med. Hypotheses 119 (2018) 14–17.
[9] Y. Wang, X. Zhang, M. Duan, C. Zhang, K. Wang, L. Feng, L. Song, S. Wu, X. Chen, Identification of potential biomarkers associated with acute myocardial infarction by weighted gene coexpression network analysis, Oxid. Med. Cell. Longev. 2021 (2021), 5553811.
[10] M.E. Ritchie, B. Phipson, D. Wu, Y. Hu, C.W. Law, W. Shi, G.K. Smyth, Limma powers differential expression analyses for RNA-sequencing and microarray studies, Nucleic Acids Res. 43 (7) (2015) e47.
[11] A.M. Newman, C.L. Liu, M.R. Green, A.J. Gentles, W. Feng, Y. Xu, C.D. Hoang, M. Diehn, A.A. Alizadeh, Robust enumeration of cell subsets from tissue expression profiles, Nat. Methods 12 (5) (2015) 453–457.
[12] S. Sha, L. Si, X. Wu, Y. Chen, H. Xiong, Y. Xu, W. Liu, H. Mei, T. Wang, M. Li, Prognostic analysis of cuproptosis-related gene in triple-negative breast cancer, Front. Immunol. 13 (2022), 922780.
[13] Y. Lai, C. Lin, X. Lin, L. Wu, Y. Zhao, F. Lin, Identification and immunological characterization of cuproptosis-related molecular clusters in Alzheimer's disease, Front. Aging Neurosci. 14 (2022), 932676.
[14] P. Langfelder, S. Horvath, WGCNA: an R package for weighted correlation network analysis, BMC Bioinf. 9 (2008) 559.
[15] S.G. Kang, S.E. Cho, Neuroimaging biomarkers for predicting treatment response and recurrence of major depressive disorder, Int. J. Mol. Sci. 21 (6) (2020).
[16] M.H. Trivedi, Major depressive disorder in primary care: strategies for identification, J. Clin. Psychiatry 81 (2) (2020).
[17] J. Slupski, W.J. Cubala, N. Gorska, A. Slupska, M. Galuszko-Wegielnik, Copper and anti-anhedonic effect of ketamine in treatment-resistant depression, Med. Hypotheses 144 (2020), 110268.
[18] R.S. Duman, Depression: a case of neuronal life and death? Biol. Psychiatr. 56 (3) (2004) 140–145.
[19] J. Zhang, S. Xie, Y. Chen, X. Zhou, Z. Zheng, L. Yang, Y. Li, Comprehensive analysis of endoplasmic reticulum stress and immune infiltration in major depressive disorder, Front. Psychiatr. 13 (2022), 1008124.
[20] J. Garrosa-Jimenez, Y. Sanchez Carro, M.C. Ovejero-Benito, E. Del Sastre, A.G. Garcia, M.G. Lopez, P. Lopez-Garcia, M.F. Cano-Abad, Intracellular calcium and inflammatory markers, mediated by purinergic stimulation, are differentially regulated in monocytes of patients with major depressive disorder, Neurosci. Lett. 765 (2021), 136275.
[21] M.A. Alvarez-Mon, A.M. Gomez-Lahoz, A. Orozco, G. Lahera, M.D. Sosa-Reina, D. Diaz, A. Albillos, J. Quintero, P. Molero, J. Monserrat, M. Alvarez-Mon, Blunted expansion of regulatory T lymphocytes is associated with increased bacterial translocation in patients with major depressive disorder, Front. Psychiatr. 11 (2020), 591962.
[22] R. Aronica, P. Enrico, L. Squarcina, P. Brambilla, G. Delvecchio, Association between Diffusion Tensor Imaging, inflammation and immunological alterations in unipolar and bipolar depression: a review, Neurosci. Biobehav. Rev. 143 (2022), 104922.
[23] J. Tan, C. Ma, C. Zhu, Y. Wang, X. Zou, H. Li, J. Li, Y. He, C. Wu, Prediction models for depression risk among older adults: systematic review and critical appraisal, Ageing Res. Rev. (2022), 101803.
[24] C.M. Hatton, L.W. Paton, D. McMillan, J. Cussens, S. Gilbody, P.A. Tiffin, Predicting persistent depressive symptoms in older adults: a machine learning approach to personalised mental healthcare, J. Affect. Disord. 246 (2019) 857–860.
[25] Z. Xu, Q. Zhang, W. Li, M. Li, P.S.F. Yip, Individualized prediction of depressive disorder in the elderly: a multitask deep learning approach, Int. J. Med. Inf. 132 (2019), 103973.
[26] H. Kim, S. Lee, S. Lee, S. Hong, H. Kang, N. Kim, Depression prediction by using ecological momentary assessment, actiwatch data, and machine learning: observational study on older adults living alone, JMIR Mhealth Uhealth 7 (10) (2019), e14149.
[27] Y. Xu, C. Her, VBP1 facilitates proteasome and autophagy-mediated degradation of MutS homologue hMSH4, Faseb. J. 27 (12) (2013) 4799–4810.
[28] T.I. Chiang, Y.Y. Hung, M.K. Wu, Y.L. Huang, H.Y. Kang, TNIP2 mediates GRbeta-promoted inflammation and is associated with severity of major depressive disorder, Brain Behav. Immun. 95 (2021) 454–461.
[29] C.W. Fell, A. Hagelkruys, A. Cicvaric, M. Horrer, L. Liu, J.S.S. Li, J. Stadlmann, A.A. Polyansky, S. Mereiter, M.A. Tejada, et al., FIBCD1 is an endocytic GAG receptor associated with a novel neurodevelopmental disorder, EMBO Mol. Med. 14 (9) (2022), e15829.
[30] C. Deneubourg, M. Ramm, L.J. Smith, O. Baron, K. Singh, S.C. Byrne, M.R. Duchen, M. Gautel, E.L. Eskelinen, M. Fanto, H. Jungbluth, The spectrum of neurodevelopmental, neuromuscular and neurodegenerative disorders due to defective autophagy, Autophagy 18 (3) (2022) 496–517.
[31] A. Tripathi, G. Scaini, T. Barichello, J. Quevedo, A. Pillai, Mitophagy in depression: pathophysiology and treatment targets, Mitochondrion 61 (2021) 1–10.
[32] J. Gao, Y. Liao, M. Qiu, W. Shen, Wnt/beta-Catenin signaling in neural stem cell homeostasis and neurological diseases, Neuroscientist 27 (1) (2021) 58–72.